

# Small-signal modulation characteristics for 1.5 $\mu\text{m}$ lattice-matched InGaNaNs/GaAs and InGaAs/InP quantum well lasers

WOON-HO SEO<sup>1</sup>, CANICE O'BRIEN<sup>2</sup>, JOHN F. DONEGAN<sup>2,\*</sup>,  
YOONSEOK LEE<sup>1</sup> AND GIL-HO KIM<sup>1</sup>

<sup>1</sup>*Department of Electronic and Electrical Engineering, Sungkyunkwan University, 440-746 Korea*

<sup>2</sup>*Semiconductor Photonics Group, Department of Physics, Trinity College Dublin, Dublin2, Ireland*

(\*author for correspondence: E-mail: jdonegan@tcd.ie)

Received 8 March 2004; accepted 12 October 2004

**Abstract.** The small-signal modulation characteristics of 1.5  $\mu\text{m}$  lattice-matched InGaNaNs/GaAs and InGaAs/InP quantum well lasers and their temperature dependence have been calculated. It is found that the maximum bandwidth of the InGaNaNs/GaAs quantum well lasers is about 2.3 times larger than that of the InGaAs/InP quantum well lasers due to the high differential gain which results from the large electron effective mass in the dilute nitride system. The slope efficiency for the 3 dB bandwidth as a function of optical density is twice as large for InGaNaNs/GaAs as for InGaAs/InP quantum well lasers.

**Key words:** 3 dB bandwidth, semiconductor quantum wells, small signal modulation

## 1. Introduction

Recently, the InGaNaNs material system has drawn much attention as light sources for optical communication and optical inter-connection systems (Kondow *et al.* 1997). In addition, the large refractive index difference of  $\lambda/4$  layers in this GaAs-based system makes it possible to fabricate efficient monolithic Bragg reflectors. Furthermore, the larger conduction band offset and larger electron effective mass of InGaNaNs/GaAs materials than those of InGaAs(P)/InP lead to a stronger electron confinement which should result in an improved high-temperature performance. Many successful operations of ridge waveguides (Ha *et al.* 2002) distributed-feedback (Reinhardt *et al.* 2000), and vertical-cavity surface-emitting lasers, (Coldren *et al.* 2000) with InGaNaNs as active layers have been reported. For high-speed optical communication, direct modulation of the laser diodes is essential. Therefore it is important to investigate the dynamic properties of the laser diodes and to understand the modulation characteristics, especially in this new material system. Presently, many experimental results are reported for lasers in 1.3  $\mu\text{m}$

wavelength region and now the challenge is directed to the achievement of 1.5  $\mu\text{m}$  wavelength lasing.

In this paper, theoretical analysis of the modulation characteristics of 1.5  $\mu\text{m}$  lattice-matched InGaNaNs/GaAs and InGaAs/InP quantum well (QW) lasers is presented. In addition, their thermal properties in the high gain situation are presented. The lattice-matched conditions for 1.5  $\mu\text{m}$  InGaNaNs/GaAs QW are determined based on the known experimental results in the 1.3  $\mu\text{m}$  range. There are as yet no experimental gain spectra at 1.5  $\mu\text{m}$ . However, the simple interpolations found when varying the nitrogen concentration suggest that an enhanced electron effective mass would also be found at 1.5  $\mu\text{m}$ . This enhanced effective mass is crucial to the gain and differential gain spectra in the InGaNaNs system.

## 2. Theoretical model

Lattice-matched  $\text{In}_{0.53}\text{Ga}_{0.47}\text{As}/\text{InP}$  and  $\text{In}_{0.1}\text{Ga}_{0.9}\text{N}_{0.036}\text{As}_{0.964}/\text{GaAs}$  single 7 nm QW lasers are considered. The lattice-matched conditions for InGaNaNs QW are obtained by the application of the band anti-crossing model and Vegard's law for the known experimental results. The equations and parameters for the band anti-crossing model are presented in the author's previous paper (Seo and Donegan 2003). For the characterization of the temperature dependencies, the Varshni's relations are used. Within the band anti-crossing model, although there is no direct coupling between the nitrogen band and the valence bands, there is an indirect interaction through the coupling with the conduction band (Shan *et al.* 1999). Including the conduction–valence band interaction with the spin degenerate nitrogen band, a  $10 \times 10$  effective mass Hamiltonian is used for the energy band structure calculations of the InGaNaNs/GaAs QWs. A microscopic theory based on semiconductor Bloch equations are used for gain calculations and the carrier-carrier scattering is treated within the quantum kinetic scheme to explain the line broadening (Lindberg and Koch 1988; Binder *et al.* 1992). Fig. 1 shows a comparison of the gain in the InGaAsN and the InGaAs systems. It is obvious that the InGaAsN system provides a much larger gain for a particular carrier density. This is due to the higher effective electron mass which leads to a much better match of the densities of states in the conduction and valence bands of the InGaAsN materials.

Using rate equations and nonlinear gain saturation, the small signal frequency response function is given by

$$R_{\text{mod}}(\omega) = \left( \frac{\Gamma \tau_p}{qd} \right) \frac{\omega_r^2}{\sqrt{(\omega^2 - \omega_r^2)^2 + \omega^2 \gamma^2}}$$

where the damping factor is defined as

$$\gamma = Kf_r^2 + \frac{1}{\tau}$$

and the  $K$  factor is given by

$$K = 4\pi^2 \left( \tau_p + \frac{\varepsilon}{vg'} \right)$$

where  $\tau_p$ ,  $\tau$ ,  $f_r$ ,  $g'$ ,  $\Gamma$ , and  $\varepsilon$  are photon lifetime, carrier lifetime, resonance frequency, differential gain, optical confinement factor, gain suppression coefficient, and the frequency  $\omega_r = 2\pi f_r$ , respectively (Chuang 1995).

### 3. Results and discussion

In the numerical calculations,  $\tau_p$ ,  $\tau$ ,  $\Gamma$ , and  $\varepsilon$  are set equal to 1.5 ps, 1.0 ns, 0.1, and  $3.0 \times 10^{-23} \text{ m}^3$ , respectively for both material systems. For the first three parameters, this is a very good approximation as these values are typical of quantum well heterostructure lasers and we will discuss the  $\varepsilon$  parameter further below. Fig. 2 shows the small-signal frequency response of InGaAsN/GaAs and InGaAs/InP QW lasers with different optical densities at a temperature of 300 K. At the same optical density, the bandwidth of InGaAsN/GaAs QW lasers is larger than that of InGaAs/InP QW lasers and also the amount of increase with the optical density increase is enhanced in the former system. The differential gains of the two systems are presented in Fig. 3 as a function of temperature at a peak gain of  $2500 \text{ cm}^{-1}$ . InGaAsN

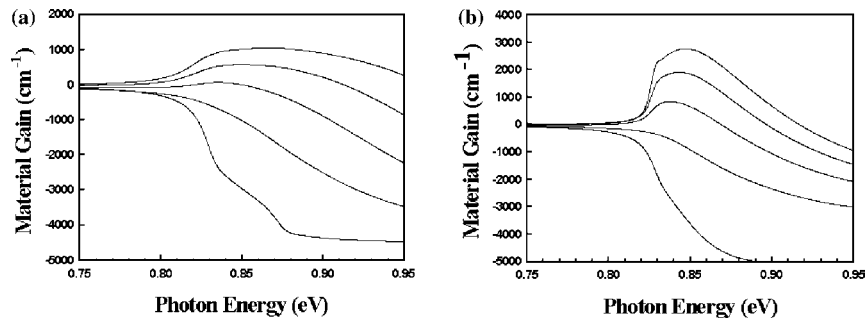


Fig. 1. Comparison of gain spectra in InGaAs/InP and InGaAsN/GaAs quantum well materials with a 7 nm quantum well width. (a) In<sub>0.53</sub>Ga<sub>0.47</sub>As/InP at carrier densities of 0.1, 1, 2, 3,  $4 \times 10^{18} \text{ cm}^{-3}$ . (b) In<sub>0.1</sub>Ga<sub>0.9</sub>N<sub>0.036</sub>As<sub>0.964</sub>/GaAs at carrier densities of 0.1, 1, 2, 3,  $4 \times 10^{18} \text{ cm}^{-3}$ .

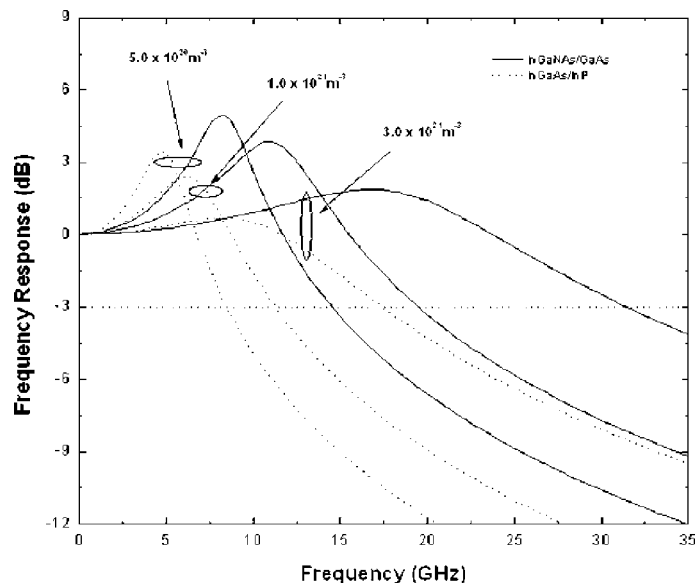


Fig. 2. Frequency responses of InGaNaS/GaAs QW (solid lines) and InGaAs/InP QW (dotted lines) at a temperature of 300 K.

QW lasers have a much larger differential gain over the temperature range from 300 to 360 K. The larger differential gain of InGaNaS is due to the enhanced electron effective mass which is  $0.104m_0$  and about 2.4 times larger than that of InGaAs (1.2 times larger for the hole effective mass). This gives a better density of states match between conduction band and valence band

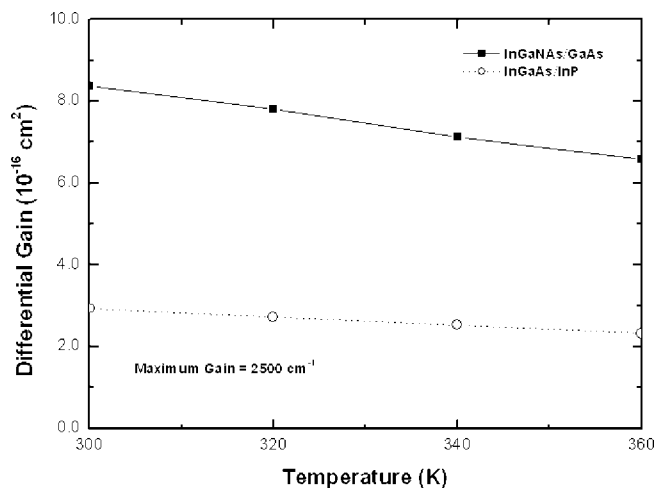


Fig. 3. Temperature dependence of differential gains for InGaNaS/GaAs QW (solid line with solid squares) and InGaAs/InP QW (dotted line with open circles) at the peak gain of  $2500\text{ cm}^{-1}$ .

which leads to high differential gain. The enhanced electron effective mass comes from the strong interaction between the conduction band and a narrow resonant band formed by the nitrogen states. In Fig. 4a the temperature dependence of  $K$ -factors for both InGaNaNs/GaAs and InGaAs/InP QW lasers are presented. The  $K$ -factor of InGaNaNs lasers is 0.225 ns and about 2.5 times smaller than that of InGaAs lasers at a temperature of 300 K which gives a maximum resonance frequency of 39.4 GHz (16.7 GHz for InGaAs/

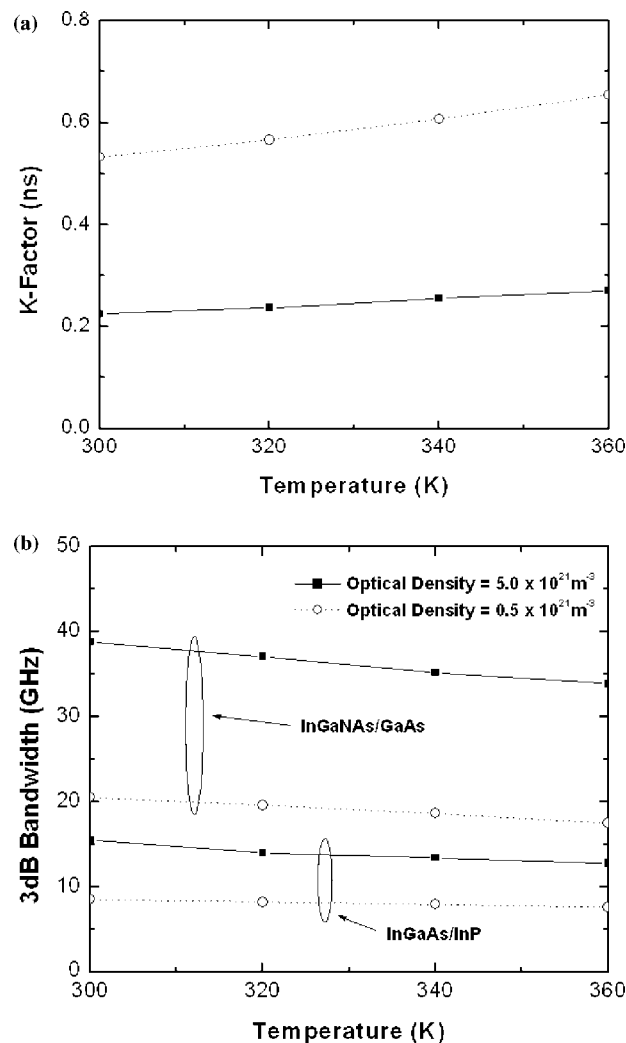


Fig. 4. (a)  $K$ -factors as a function of temperature for InGaNaNs/GaAs QW (solid line with solid squares) and InGaAs/InP QW (dotted line with open circles). (b) Temperature dependence of 3 dB bandwidth for InGaNaNs/GaAs and InGaAs/InP QWs at the optical density of  $0.5 \times 10^{21} \text{ m}^{-3}$  (solid line with solid squares) and of  $5.0 \times 10^{21} \text{ m}^{-3}$  (dotted line with open circles).

InP QW lasers) using the 3 dB cutoff condition,  $f_{r,\max} = \frac{2\pi\sqrt{2}}{K}$ . This is also due to the enhanced differential gain in the InGaNaNs system. For the temperature range of 300–360 K, the temperature dependence of the 3 dB modulation bandwidth of InGaAs/InP QW lasers is smaller than that of InGaNaNs/GaAs QW lasers, but the values are much larger for the InGaNaNs system as shown in Fig. 4b. Also, the increasing rate of the 3 dB modulation bandwidth for InGaNaNs with the injection current (that is, optical density) is twice as large as that for InGaAs resulting in a higher modulation current efficiency factor (the slope of modulation bandwidth as a function of injection current). The large conduction band offset (deep quantum well) in the InGaNaNs/GaAs QW increases the electron escape time which leads to the decrease in damping rate (Tsai *et al.* 1997) and gives better high-temperature performance in high-speed modulation. In this paper, the same gain suppression coefficient  $\varepsilon$  is used for both systems and the temperature-independence is assumed as was shown by the experiments for 1.3  $\mu\text{m}$  InGaAsP/InP lasers (Ishikawa *et al.* 1992). There are no available experimental results to determine the gain suppression coefficient of InGaNaNs materials to date, but the stronger confinement of electrons due to the enhanced conduction band offset should result in a lower gain suppression coefficient as shown by the experiments for InGaAs/InAlGaAs QW lasers in comparison with InGaAs/InGaAsP QW lasers (Grabmaier *et al.* 1991). This will further increase the difference of the modulation bandwidth between the InGaNaNs/GaAs and InGaAs/InP QW lasers. It is therefore a reasonable assumption that the  $\varepsilon$  coefficient of InGaAsN lasers will be much less than the InGaAsP lasers. Our use of the same value is therefore a conservative position and the modulation characteristics that will be observed in future devices will likely be better than those given in this paper.

#### 4. Conclusion

It is demonstrated that the lattice-matched InGaNaNs/GaAs QW lasers have enhanced high-speed modulation characteristics when compared with conventional InGaAs/InP QW lasers for a wavelength of 1.5  $\mu\text{m}$ . This is mainly due to the large differential gain in the InGaNaNs system resulting from the larger conduction band effective mass. The maximum 3 dB modulation bandwidth of 39.4 GHz (2.3 times larger than that of the InGaAs/InP system) is achieved by assuming that a gain suppression coefficient of  $3.0 \times 10^{-23} \text{ m}^3$  at a temperature of 300 K. Using multiple quantum wells and the introduction of the lattice-mismatch in the InGaNaNs material system can further improve the modulation characteristics. The considerations in this article will give some useful directions for the design of 1.5  $\mu\text{m}$  lasers in the InGaNaNs material system.

### Acknowledgments

The authors are grateful to James O’Gorman for valuable discussions and suggestions. This work was supported in Korea by the National Research and Development Project for Nano Science and Technology (contract No. N11-0212-04-0003) of NOST. The work was supported by the Phase II projects of Enterprise Ireland under the Programmes in Advanced Technologies in Ireland.

### References

- Binder, R., D. Scott, A.E. Paul, M. Lindberg, K. Henneberger and S.W. Koch. *Phys. Rev. B* **45** 1107, 1992.
- Chuang, S.L. *Physics of Optoelectronic Devices*, Wiley Interscience, 1995.
- Coldren, C.W., M.C. Larson, S.G. Spruytte and J.S. Harris. *Electron. Lett.* **36** 951, 2000.
- Grabmaier, A., A. Hangleiter, G. Fuchs, J.E.A. Whiteway and R.W. Glew. *Appl. Phys. Lett.* **59** 3024, 1991.
- Ha, W., V. Gambin, M. Wistey, S. Bank, S. Kim and J.S. Harris, Jr. *IEEE Photonics Technol. Lett.* **14** 591, 2002.
- Ishikawa, M., T. Fukushima, R. Nagarajan and J.E. Bowers. *Appl. Phys. Lett.* **61** 396, 1992.
- Kondow, M., T. Kitani, S. Nakatsuka, M.C. Larson, K. Nakahara, Y. Yazawa, M. Okai and K. Uomi. *IEEE J. Sel. Top. Quantum Electron.* **3** 719, 1997.
- Lindberg, M. and S.W. Koch. *Phys. Rev. B* **38** 3342, 1988.
- Reinhardt, M., M. Fischer, M. Kamp, J. Hofmann and A. Forchel. *IEEE Photonics Technol. Lett.* **79** 239, 2000.
- Seo, W.H. and J.F. Donegan. *Appl. Phys. Lett.* **82** 505, 2003.
- Shan, W., W. Walukiewicz, J.W. AgerIII, E.E. Haller, J.F. Geisz, D.J. Friedman, J.M. Olson and S.R. Kurz. *Phys. Rev. Lett.* **82** 1221, 1999.
- Tsai, C.Y., F.P. Shih, T.L. Sung, T.Y. Wu and C.H. Chen. *IEEE J. Quantum Electron.* **33** 2084, 1997.